



Morgan, K. et al. (2020) Oxygen plasma treated substrates and specific nanopattern promote early differentiation and function of HepaRG progenitor cells. *Tissue Engineering Part A*, 26(19-20), pp. 1064-1076. (doi: [10.1089/ten.TEA.2019.0241](https://doi.org/10.1089/ten.TEA.2019.0241)).

This is the author's final accepted version.

There may be differences between this version and the published version. You are advised to consult the publisher's version if you wish to cite from it.

<http://eprints.gla.ac.uk/215553/>

Deposited on: 06 May 2020

Enlighten – Research publications by members of the University of Glasgow
<http://eprints.gla.ac.uk>

Oxygen plasma treated substrates and specific nanopattern promote early differentiation and function of HepaRG progenitor cells

Katie Morgan¹, Anna Bryans¹, Filip Brzeszczyński¹, Kay Samuel², Philipp Treskes¹, Austin Koh, Joanna Brzeszczyńska^{1,3}, Steven D Morley¹, Peter C Hayes¹, Nikolaj Gadegaard^{*4}, Leonard J Nelson^{*5} and John N Plevris^{*1}

*equal last authors

¹Hepatology Laboratory, University of Edinburgh, Royal Infirmary of Edinburgh, Edinburgh, United Kingdom; ²Scottish National Blood Transfusion Service, Advanced Therapeutics, The Jack Copland Centre, 52 Research Avenue North, Edinburgh, United Kingdom; ³ Department of Molecular Biophysics, University of Lodz, Lodz, Poland, ⁴Division of Biomedical Engineering, University of Glasgow, Glasgow G12 8LT, United Kingdom. ⁵Institute for BioEngineering (IBioE), School of Engineering, The University of Edinburgh, The Kings Buildings, Edinburgh EH9 3JL United Kingdom;

Corresponding Author:

Katie Morgan

Hepatology Laboratory

University of Edinburgh

Royal Infirmary of Edinburgh,

Chancellor's Building

49 Little France Crescent

Edinburgh EH16 4SB (UK)

07725216902

Degree: PhD

Katie.Morgan@ed.ac.uk

Contributing Authors:

Anna Bryans

Hepatology Laboratory

University of Edinburgh

Royal Infirmary of Edinburgh,

Chancellor's Building

49 Little France Crescent

Edinburgh EH16 4SB (UK)

07824902425

Degree: MBChB

s1201949@sms.ed.ac.uk

Filip Brzeszczyński

Hepatology Laboratory

University of Edinburgh

Royal Infirmary of Edinburgh,

Chancellor's Building

49 Little France Crescent

Edinburgh EH16 4SB (UK)

07910142536

Degree: MBChB

ff.brzeszczynski@gmail.com

Kay Samuel

Scottish National Blood Transfusion Service

Advanced Therapeutics

The Jack Copland Centre

52 Research Avenue North,

Edinburgh

07905199106

Degree: BSc

k.samuel@ed.ac.uk

Philipp Treskes

Hepatology Laboratory

University of Edinburgh

Royal Infirmary of Edinburgh,

Chancellor's Building

49 Little France Crescent

Edinburgh EH16 4SB (UK)

+4915730127369

Degree PhD

p.treskes@gmail.com

Joanna Brzeszczyńska

Hepatology Laboratory

University of Edinburgh

Royal Infirmary of Edinburgh,

Chancellor's Building

49 Little France Crescent

Edinburgh EH16 4SB (UK)

07910142536

Degree Phd

joanna.brzeszczynska@googlemail.com

Steven D Morley

Hepatology Laboratory

University of Edinburgh

Royal Infirmary of Edinburgh,

Chancellor's Building

49 Little France Crescent

Edinburgh EH16 4SB (UK)

0131-242-6215

Degree: PhD

steve.morley@ed.ac.uk

Professor Peter C Hayes

Hepatology Laboratory

University of Edinburgh

Royal Infirmary of Edinburgh,

Chancellor's Building

49 Little France Crescent

Edinburgh EH16 4SB (UK)

01315361000

Degree: PhD

p.hayes@ed.ac.uk

Professor Nikolaj Gadegaard

Division of Biomedical Engineering,

University of Glasgow,

Glasgow G12 8LT

01413305243

Degree: PhD

Nikolaj.Gadegaard@Glasgow.ac.uk

Leonard J Nelson

Institute for BioEngineering (IBioE),

School of Engineering,

The University of Edinburgh,

The Kings Buildings,

Edinburgh EH9 3JL

07792667425

Degree: PhD

l.nelson@ed.ac.uk

Professor John N Plevris

Hepatology Laboratory

University of Edinburgh

Royal Infirmary of Edinburgh,

Chancellor's Building

49 Little France Crescent

Edinburgh EH16 4SB (UK)

01312421631

Degree: PhD

J.plevris@ed.ac.uk

Key words: Nanopattern, oxygen plasma, HepaRG, early differentiation, progenitor cells

Conflict of interest: The authors have no conflict of interest to declare with respect to this manuscript.

Financial support: The Hepatology Laboratory was supported by the BBSRC (BB/L023687/1) during the period of this research.

Authors' contributions:

Katie Morgan – Writing of manuscript, data curation, formal analysis, investigation, methodology, project administration

Anna Bryans – contribution to manuscript, data curation, formal analysis, investigation, methodology

Filip Brzeszczyński – editing of manuscript, data curation, formal analysis, investigation, methodology

Kay Samuel – editing of manuscript, formal analysis, methodology

Philipp Treskes- editing of manuscript, methodology, funding acquisition

Steve Morley – editing of manuscript, methodology, funding acquisition

Joanna Brzeszczynska – editing of manuscript, methodology, data curation, supervision, formal analysis

Peter Hayes – Funding acquisition, supervision

Nikolaj Gadegaard- conceptualisation, funding acquisition, editing of manuscript, methodology, formal analysis, project administration, supervision

Leonard J Nelson – conceptualisation, funding acquisition, methodology, formal analysis, project administration, supervision

John Plevris – funding acquisition, editing of manuscript, formal analysis, supervision

Abstract

Fully differentiated HepaRG™ cells are the hepatic cell line of choice for *in vitro* work in toxicology and drug trials. They are derived from a hepatoblast-like progenitor (HepaRG™-P) that differentiates into a co-culture of hepatocyte-like and cholangiocyte-like cells. This process that requires 2 weeks of proliferation followed by 2 weeks of differentiation using dimethylsulfoxide (DMSO) can be time consuming and costly. Identifying a method to accelerate HepaRG™-Ps towards a mature lineage would save both time and money. The ability to do this in the absence of DMSO would remove the possibility of confounding toxicology results caused by DMSO induction of CYP pathways.

It has been shown, that tissue culture substrates play an important role in the development and maturity of a cell line, and this is particularly important for progenitor cells, which retain some form of plasticity.

Oxygen plasma treatment is used extensively to modify cell culture substrates. There is also evidence that patterned rather than planar surfaces have a positive effect on proliferation and differentiation. In this study, we compared the effect of standard tissue culture plastic (TCP), oxygen plasma treated (OPC), and nanopatterned surfaces (NPS) on early differentiation and function of HepaRG™-P cells.

Since NPS were oxygen plasma treated we initially compared the effect of TCP and OPC to enable comparison between all 3 culture surfaces using OPC as control to assess if patterning further enhanced early differentiation and functionality. The results show that HepaRG™-P's grown on OPC substrate exhibited earlier differentiation, proliferation and function compared to TCP. Culturing HepaRG™-P's on OPC with the addition of NPS did not confer any additional advantage. In conclusion, OPC surface appeared to enhance hepatic differentiation and functionality and could replace traditional methods of differentiating HepaRG-P cells into fully differentiated and functional HepaRGs earlier than standard methods.

Impact statement

We show significantly earlier differentiation and function of HepaRG progenitor cells when grown in DMSO-free medium on oxygen plasma substrates vs standard tissue culture plastic. Further investigation showed that nanopatterning of oxygen plasma substrates did not confer any additional advantage over smooth oxygen plasma, though one pattern (DSQ120) showed comparable early differentiation and function.

Introduction

Fully differentiated HepaRG™ cells have been recognised as a ‘surrogate’ of primary human hepatocytes (PHHs) for use in pharmacological applications.^{1,2} They are an attractive and more physiologically relevant model for evaluating toxicity of compounds as they express phase I and II metabolism, and have superior cytochrome P450 (CYP) activity compared to other hepatic cell lines.^{1,2} The HepaRG™ progenitor (HepaRG™-P) line represents a bi-potent culture which retains plasticity, and can be differentiated into a co-culture of cholangiocyte-like and hepatocyte-like cells over a 28 day process of proliferation and differentiation (**Figure 1**). By pushing cells, already committed to a specific lineage, they are more likely to develop and maintain a differentiated phenotype.^{3,4} During weeks 1 and 2, cells proliferate in dimethyl sulfoxide (DMSO) free media followed by DMSO+ media for a further two weeks in order to promote and maintain differentiation. However, while the effect of DMSO produces a stable differentiated co-culture, it can induce CYP pathways that could mask specific drug-induced CYP activity or cause unintended induction or inhibition effects in toxicity assays.⁵ Therefore, finding a method whereby cells can differentiate and maintain their mature phenotype without DMSO would be beneficial for toxicity studies.

Cell culture substrates

Within this project it was our intention to specifically assess whether topology of a surface can be used to improve/promote growth and differentiation. Oxygen plasma has been used in the production of tissue culture plates since the 1970s.⁶ Though we have found no studies where OPC treatment has been reported to impact differentiation or function of hepatocytes, it has been shown that oxygen plasma treatment of surfaces increased cellular adhesion, spreading and growth rate compared to untreated control.^{7,8} Therefore, the morphology of HepaRG™-P's grown on OPC was compared with those grown on standard tissue culture plastic (TCP), with a view to use OPC as an internal control to assess the effect of nanopatterned substrates (NPS) on induction of differentiation.

NPS are increasingly being used in tissue engineering as they appear to promote differentiation of stem/progenitor cells.^{9,10} Finding an NPS that would advance the timing of differentiation of HepaRG™-Ps without the need for DMSO would be potentially more cost effective, and eliminate disadvantages associated with the use of DMSO in terms of metabolic activity.

The aims of this study were based on the following two hypotheses. First, that proliferation and differentiation of HepaRG™-Ps would be comparable on both TCP and OPC substrates, such that OPC would be an internal control when assessing NPS. The second hypothesis was that HepaRG™-P cells grown on NPS would proliferate faster, differentiate earlier and outperform cells grown on either TCP or OPC.

Materials and methods

Cell culture

HepaRG™ Progenitors were cultured in medium consisting of William's E Medium + GlutaMAX™ (32551-020, Life Technologies, Paisley, UK) and Biopredic's proprietary growth medium supplement (ADD711077 Growth Medium Supplement, Biopredic Int'l, Rennes, France) without dimethylsulfoxide for the duration of experimentation. Prior to seeding the HepaRG™-P, OPC and NPS plates were wetted with 100µl of media at room temperature for 1 hour. This ensured better adherence of cells to the surface substrate, and also confirmed that there was no leakage on the plate.

Surface treatment of tissue culture substrate

There are various surface treatments available to create an adhesive hydrophilic surface. The two main types of treatment are oxygen plasma and corona treatments. In this study, oxygen plasma treatment was chosen due to the controlled conditions and high reproducibility of this technique. For all experiments an oxygen plasma treatment of 40W for 30s was used. To allow the investigation to focus on surface architectures which were not detrimental to cell attachment and/or differentiation HepaRG™-P cells were cultured on treated surfaces for assessment of adhesion and morphology as compared to TCP by microscopy.

Nanopattern plates

NPS were produced [at the University of Glasgow](#) by electron beam lithography [as detailed in Huethorst et al., 2020](#).¹¹ A patterned silicon chip was manufactured and a

nickel shim was created based on this chip and used at high pressure to print the various nanopatterns onto a molten polymer. Once hardened this polymer was fixed within a plate framework and treated with oxygen plasma before use. In the first instance, single OPC wells were prepared by omitting nanopattern steps, applying only oxygen plasma treatment.

Subsequently, twenty-one different patterns consisting of both organised and disorganised arrays of pits were applied to OPC treated surfaces. Spacing of pits on disorganised (DSQ) patterns had different degrees of disorder which allowed for a cursory assessment of nanotopographical sensitivity of the cells¹¹. A gradient of 10nm to 150nm was used alongside ordered patterns and are indicated within the name of each well i.e. DSQ20, DSQ30, DSQ40 and so on (**Figure 2**). With 21 permutations of pattern a set of criteria for evaluation of what is good vs what is a bad pattern was established. A good pattern was defined as showing adherent cells with clear edges, cells must reach confluency within 7-10 days and ideally show some commitment to a hepatocyte lineage by exhibiting binucleation and/or formation of bile ducts. Patterns where cells did not adhere, reach confluency, or retained jagged edges were disregarded. These criteria were assessed via daily microscopy from 3 independent researchers to decide upon a pattern or set of patterns for further investigation using the toolkit comprised of microscopy, immunostaining, viability, total protein and qRTPCR of functional and phenotypical expression.

Microscopy

All phase and fluorescent imaging was performed with an EVOS Auto FL™ imaging platform (Thermo Scientific, Massachusetts, USA). Image magnification is specified on a figure by figure basis.

The EVOS Auto FL™ has the ability to set a 'beacon', a customized focal point, that can be saved as a routine so the microscope can return to the same spot to take consecutive pictures over time. The routine is saved and can be run automatically or manually. Two beacons were set per well, at random, to observe morphology and adhesion.

Immunocytochemistry

Cells were washed with Tris-Buffered Saline (TBS) (TBS; T6664; Sigma-Aldrich, Dorset, UK) for 2 minutes prior to fixation in 4% formaldehyde (28908, Thermo Scientific, Massachusetts, USA) at 4°C for 1 hour. Cells were then washed with TBS and permeabilized with 0.1% Triton X 100 (85111, ThermoFisher, Massachusetts, USA) for 30 minutes. Following a further TBS wash, samples were blocked with 5% goat serum (G6767; Sigma-Aldrich, Dorset, UK) for 1 hour. Primary antibody was then added and incubated at 4°C overnight (Primary antibodies listed in **Table 1**) after which, cells were washed in TBS on a shaker for approximately 20 minutes and then washed again before adding secondary antibody, Hoescht and phalloidin. Secondary antibody incubation was at 4°C for 4 to 24 hours, depending on antibody, and three further wash steps were performed after incubation and before microscopy.

Secondary staining

Secondary detecting antibody goat-anti-rabbit Alexa Fluor 488 (11034, Life Technologies, UK 1:1000 dilution) was combined with Hoescht 33342 (HS1492; Life Technologies, UK, 10µg/mL) for immunostaining of Z-O1, Sox9 and HNF4α.

Viability & metabolic proficiency assays

PrestoBlue™ 10% (v/v) (A-13262; Life Technologies Paisley, UK) was added to Phosphate Buffered Solution with calcium chloride and magnesium chloride (PBS+) (D8662, Sigma Aldrich, Dorset, UK, 500ml) in a 1:10 solution. Cells were washed with PBS+ prior to addition of 100µl PrestoBlue™ suspension. After incubation for 30 minutes at room temperature, the fluorescent signal was read on a GloMax-Multi™+ Microplate Multimode Reader (Promega, Southampton, UK) using a white walled and bottomed 96 well plate.

Post PrestoBlue™ measurement, the supernatant was discarded, and cells rinsed with PBS+ before addition of Promega Cell Titer Glo™ ATP lysis buffer to determine total cellular ATP levels using the CellTiter-Glo™ Luminescent Cell Viability Assay (G7570; Promega, Southampton, UK), as per vendor's instructions. Briefly, incubation with substrate at room temperature for 20 minutes was followed by adding ATP detection solution and bioluminescent signals were detected on a GloMax-Multi™+ Microplate Multimode Reader (Promega, Southampton, UK) using white walled and bottomed plates. PrestoBlue™ and ATP assays were always carried out on the same culture so data would be directly comparable.

Pierce BCA total protein analysis

Pierce™ BCA protein assay kit (ThermoFisher.com catalogue number 23225, 500ml.

[https://www.thermofisher.com/order/catalog/product/23227?SID=srch-srp-](https://www.thermofisher.com/order/catalog/product/23227?SID=srch-srp-23227#/23227?SID=srch-srp-23227)

[23227#/23227?SID=srch-srp-23227](https://www.thermofisher.com/order/catalog/product/23227?SID=srch-srp-23227#/23227?SID=srch-srp-23227)) was used to measure total protein of HepaRG-

P™ day 7 cells grown on TCP, OPC and DSQ120 cell culture substrates. Albumin standards (BSA) were made according to manufacturer's specifications. Cells were washed once with PBS+ before addition of lysis buffer (100µl per well) and put onto a cell shaker for 30 minutes.

A 25µl aliquot from each well was then transferred to a clear 96 well plate and 200µl of working reagent was added for incubation at 37°C for 30 minutes. This reaction measures proteins by colorimetric detection of copper using bicinchoninic acid.

Known as the 'biuret reaction', amino acids form a blue coloured complex when they react with cupric ions. Bicinchoninic acid (BCA) is then added to develop the colour further so it can be read at 562nm. Absorbance was measured on Promega GloMax multi-well plate reader.

Molecular analysis

RNA extraction

In brief, RNA extraction was undertaken using Life Technologies RNAqueous™ kit and RNA purity/quantity was measured using Thermo Fisher NanoDrop and Agilent chip technology. Every sample was assessed on NanoDrop and a selection of samples at random were assessed on the Agilent chip.

cDNA synthesis and qRT-PCR analysis

cDNA was prepared using PrimerDesign nanoScript to RT kit and qRT-PCR was performed using PrimerDesign-validated primers and master mix on a Roche light cycler 96 system. For data normalization 12 candidate genes were analysed to identify stably expressed reference genes (RG). Results were assessed using Biogazelle geNorm software which uses raw Ct values taken from the Light Cycler 96 to rank RGs in order of stability: assigning an M value to represent stable expression and V values to suggest how many RGs should be used to create a geometric mean that gives the best stability across all experimental conditions. Graphpad Prism software was used for statistical analysis. A one way Anova and Tukey test were used to assess statistical significance between genes of interest. RNA samples were stored in -80°C and cDNA samples were stored at -20°C until processed.

Reference genes

Reference gene (RG) analysis was repeated independently three times using HepaRG™-P cells synchronized at a specific passage. Thawed cells were plated separately in order to create 3 independent technical replicates. As this experiment was carried out with 3 biological replicates, the total independent technical replicates were 9.

Based on current literature.^{12,13} 12 RGs were assessed, for use in normalizing genes of interest (GOI) for experiments using HepaRG™-P grown on different substrates.

All samples were run against 12 RGs; UBC, YWHA, SDHA GAPDH EIF4A1, B2M, TOP1, RPL13A, ATP5B, CYC1, 18s and ACTB (**Table 2**).

Statistical Analysis

Data evaluation and graphical illustration were performed with GraphPad Prism™ 5.0 and 7.0 (GraphPad Software, Inc., San Diego, CA, USA). Three technical replicates were assessed for each experimental condition across three separate experiments, unless stated otherwise, and results are presented as mean \pm SD. Appropriate statistical analysis was performed for each experiment including one-way ANOVA, t-test, multiple ANOVA and post hoc Tukey test, each detailed in individual chapters. Results were considered significant at $p < 0.05$.

Results

Morphological criteria

Initial evaluation of HepaRG™-P cell cultures on different surfaces showed that adherence and morphology on OPC and DSQ120 were comparable or improved as compared to TCP. Other NPS arrays were discounted from further study having shown no advantage over TCP or OPC.

Repeated observation of HepaRG™-P cells grown on OPC showed the emergence of cuboidal, hepatocyte-like cells (**Figure 3**) that were confluent on ~ days 6 and 7. Cells grown on TCP were not confluent at day 6, retained fibroblastic morphology, and did not show any cuboidal hepatocyte-like cells.

According to our criteria, we found only one pattern, DSQ120, which met our objectives and was used for the remainder of the study. This pattern showed early adhesion, confluency and evidence of bi-nucleation at day ~~6~~7 before any other pattern tested (**Supplementary figure 1**) Results are based on a comparison of all three substrates.

Phenotype

Gene of interest results are presented as fold-changes in gene expression relative to untreated control calculated with the $\Delta\Delta Cq$ method.

Zonular occludens 1 as a marker of polarity

One of the basic indications of hepatocyte maturity is polarisation of the cell. Zonular occludens 1 (ZO-1) is a membrane bound protein that stabilizes tight junctions by interacting with the F-actin portion of the cytoskeleton, therefore, the presence of ZO-1 localized within the membrane at cell-cell junctions is indicative of polarity.

Distinct membrane bound positive staining for ZO-1 was seen for cells cultured on OPC and DSQ120 at day 7 (**Figure 4**).

Staining was confirmed by qRT-PCR for expression of TJP1 a gene encoding for ZO-1. An 3×10^9 fold increase can be seen on OPC and 30,000 fold increase on DSQ120 at day 7 compared to TCP. (**Figure 4**).

SOX9/HNF4 α expression

Though expressed in other tissues HNF4 α and SOX9 are markers of hepatocyte and early cholangiocyte differentiation respectively. Expression of these genes were therefore used to assess maturation and differentiation of HepaRGTM-P cells into separate hepatocytes and cholangiocyte populations. Cells with early transient expression of SOX 9 are cholangiocyte-like cells. Later expression of HNF4 α identifies maturing hepatocytes. ¹⁴

When cultured on OPC substrate, expression of SOX9 was bright and well defined by day 6 which became diffuse by day 14, reaching a maximum by day 28.

TCP showed organised expression of SOX9 at day 6 which was diffuse at day 14 and reappeared at 28.

On DSQ120, SOX9 expression initially followed that seen on OPC at day 2 to 14, but returned to day 6 levels by day 28.

HNF4 α was not seen at day 2 on any substrate. By day 6, little to none was observed TCP and DSQ120 and localised staining was seen on OPC. On all substrates localised staining was apparent on days 14 and 28. (**Figure 5**).

qRT-PCR analysis of SOX9 showed no expression at any time under any condition. This analysis was repeated 3 times with 3-4 technical replicates each time. HNF4 α was present in all conditions on day 7 though there was an 80 fold increase on OPC and a 60 fold increase on DSQ120 compared to TCP control (**Figure 6**).

Function

Viability assays

Total ATP and PrestoBlue™ was measured at day 7. Total ATP data shows a significant difference between TCP and OPC ($p < 0.0008$) and TCP and DSQ120 ($p < 0.007$). However, no statistical difference was seen between any condition at day 7 in the PrestoBlue™ assay (**Figure 7**). Total protein was also measured at day 7 showing significantly higher protein levels for TCP compared to DSQ120 ($p = 0.25$) and OPC (**Figure 7**). This suggests that there was a greater number of cells on TCP, though OPC and DSQ120 had higher ATP levels.

Transferrin

Transferrin, required for transport of iron into hepatocytes, is a marker of a functional hepatocyte.¹⁵ At day 7, localized transferrin expression was more abundant on cells grown on OPC than in cells cultured on DSQ120. On TCP, cells show some diffuse and un-localised transferrin staining suggesting the protein was present, but not yet functional (**Figure 8**)

CYP3A4 activity

Mature cytochrome P450 enzymes also show functionality of hepatocytes. On day 7 CYP3A4, one of the major CYP enzymes in the metabolism of xenobiotics, was detected on OPC and DSQ120 using both qRT-PCR and immunostaining. At day 7 there was an 80 fold increase on OPC and a 60 fold increase on DSQ120 compared

to control. OPC and DSQ120 showed an abundance of CYP3A4, at this stage, not normally seen without the addition of DMSO (**Figure 9**).

Selection of reference genes

Following MIQE guidelines criteria and using geNorm software we identified a set of stably expressed reference genes appropriate for validation of gene of interest results for each gene across all experimental conditions.

(Table 3). Traditionally SD of Ct values has been used to assess stability. GeNorm software calculates gene expression stability (M value) using average pairwise variation (V value) for a gene comparing it with other tested reference genes across all experimental conditions.¹⁶ Low M values suggests high stability of expression.

Within this study, mean SD was 0.3 with a range from 0 to 0.5 in individual samples, showing mRNA low transcriptional variations (**Supplementary figure 2**). However, M values showed low stability ($M > 1$) when individual samples were assessed across all experimental conditions (**Table 3**). CYC1 was the only gene with an M value ranking < 1 , SDHA and 18S M values ranked between 1 and 1.2, and UBC, EIF4A1, GAPDH and ATP5B ranked between 1.2 and 2.5. V values which evaluate the optimum number of RGs needed for normalization of data indicated variability between sequential normalization factors was relatively high (geNorm $V > 0.15$) suggesting at least 7-8 RGs were recommended to normalize GOI (**Supplementary figure 2**). Genes with an M value higher than 1 are not stable enough for use as RG. Within this study, CYC1 was the only gene with an M value ranking less than 1, SDHA and 18S M values ranked between 1 and 1.2, and UBC, EIF4A1, GAPDH and

ATP5B ranked between 1.2 and 2.5. This confirms the need for a set of RGs, geNorm software suggested a set of 7-8 for analysis of GOI data.

The geometric mean of the top three genes (CYC1, SDHA and 18s) were therefore used as per the minimum requirement specified in the (MIQE) guidelines.¹⁷

Discussion

This study examined proliferation, differentiation and function of HepaRG™-Ps grown on various surface chemistries and patterns in DMSO-free medium. We hypothesised that HepaRG™- Ps cultured on OPC substrate in DMSO-free media would not show a difference in respect of differentiation and function from those grown on TCP. However, addition of a nanopattern to an OPC surface might promote growth and differentiation of HepaRG™-Ps in DMSO-free media, as NPS have been shown to increase proliferation and differentiation without the use of exogenous chemical signals in other models.^{9,18}

Oxygen plasma treatment

Oxygen plasma treatment is used to enhance cellular adhesion to substrates as it increases surface polar groups which improves hydrophilicity⁷, however, it was unknown if OPC would affect differentiation or function of cells. Oxygen plasma treatment is measured as wattage over time. A study by Wan et al.⁷, showed oxygen plasma treatment of 50W for 2-5 minutes increased adherence to poly (lactide-co-

glycolide) (PLGA) films, however extending treatment time increased surface roughness, reducing the number of polar groups on the surface of the PLGA, compromising adherence.⁷

While we anticipated improved adhesion using OPC, it was interesting to find that using low oxygen plasma treatment of 40W for 30 seconds alone had an effect on differentiation and function. Normally within an early HepaRG™-P culture, cholangiocyte-like cells appear elongated and thin with a single nucleus, whereas developing hepatocytes emerging later in culture appear more cuboidal, are binucleate, and have a more granular appearance. HepaRG™-Ps grown on OPC showed increased proliferation and some differentiation around day 7 indicated by a high level of confluency and appearance of cuboidal cells, not seen in those grown on standard TCP. In view of these observations, we investigated various markers of differentiation and function and compared OPC directly to TCP.

Polarity

Membrane polarity, the hallmark of an established hepatocyte culture, is maintained by the function of tight junctions that regulate passage of ions and molecules through the cell from apical to basal surfaces. Cellular distribution of ZO-1 part of the membrane bound complex regulating tight junctions is indicative of polarity.

Figure 5 shows the presence of ZO-1 in both OPC and TCP cultured cells. However, the location of this protein within the cell determines whether it is a marker of polarity. In TCP, although ZO-1 is clearly present, it remains mostly cytoplasmic and not membrane bound. This is typical of a protein undergoing translation as it migrates to its point of function, whereas on OPC, ZO-1 can be seen clearly within

the membrane where it is functional. qRT-PCR supports this observation, showing a 3×10^9 fold increase of TJP1 (the gene encoding for ZO-1) on OPC than TCP when results are presented as fold-changes in gene expression relative to untreated control. (**Figure 4**).

SOX9/HNF4 α reciprocal expression

SOX9 is an ubiquitous protein found in a variety of cell types and is known by several different names (CMD1; SRA1; CMPD1; SRXX2; SRXY10; SRYBOX9),¹⁹ it is reported as an early marker of the cholangiocyte lineage.^{20,21} HNF4 α is a member of a nuclear receptor family of transcription factors found in digestive tissue such as gut^{22,23} and liver²⁴. As the HepaRGTM-P cell line only differentiates into cholangiocytes and hepatocytes expression of SOX9 and HNF4 α can be used to identify early stage cholangiocyte and differentiated hepatocytes respectively. Sox9 was seen early in both OPC and TCP cultures, was lower by day 14 on TCP and reappeared at day 28 on TCP.

While SOX9 is known to be a marker of an early cholangiocyte lineage, it is possible that this gene has many other functions. It is believed that many genes have a degree of pleiotropy, or the ability to multitask²⁵, and It is possible that while SOX9 is a marker of early phenotype, it may have other functions at a later stage of cellular development especially since it is so well conserved across a variety of tissues.

HNF4 α is responsible for downstream regulation of many metabolic processes such as bile acid synthesis, lipid and glucose metabolism and the uptake of iron mediated by transferrin.^{24,26} *In vivo* loss of function studies using knock out mice showed loss of HNF4 α resulted in mortality.²⁴ Furthermore, acute disruption of this protein,

results in hepatosteatosis, and impacts apoptosis, cell cycle and growth factors downstream.²⁴ Expression of HNF4 α was therefore used as a marker of hepatocyte phenotype and function in assessing differentiation of HepaRG™-P's on the different treated surfaces.

To establish reciprocal expression, one would expect to see clear indication of SOX9 early in the culture (week 1-2) and no, or diffuse expression in later weeks. Whereas, HNF4 α should not be present early in the culture or should not be well established until the cells following the hepatocyte lineage become committed. At this stage it would be expected that HNF4 α would become localized and clear.

For both surface treatments, SOX 9 was present and localized in cytoplasm with a sharp and clear appearance on day 6. Around day 14 staining for SOX9 became more diffuse on OPC and DSQ120 and showed lower expression on TCP as cholangiocytes matured. qRT-PCR data suggests that there is no SOX9 expression at any time point on any condition (**Figure 6**). As qRT-PCR data quantifies total mRNA of specific genes, in this case SOX9, we could consider that the mRNA had already been translated into the protein detected by immunocytochemistry. As we show SOX9 staining clearly in all samples, this would indicate that further work is required to validate SOX9 within qRT-PCR experiments. Primers were validated by Primer Design, though, to add credence to this analysis, we would need to validate them using a cell line or tissue known to express high levels of SOX9

HNF α expression was seen on both surfaces (OPC and TCP) by day 14 and was maintained at day 28, and qRT-PCR analysis showed an 80 fold increase at day 7 of HNF4 α in cells cultured on OPC vs TCP and around a 60 fold increase in cells culture on DSQ120 vs TCP.

Viability: Total ATP and metabolic function

Within this study two biochemical assays PrestoBlue™ and total ATP were used to assess viability and metabolic function of the cells.

The Pierce BCA total protein kit was also used to quantify total protein which would correlate cell number between conditions, this also allowed for a direct comparison of metabolic proficiency assuming there was not a statistical difference.

On day 7 there was a significant increase in total ATP on OPC compared to TCP suggesting increased viability/metabolic activity of the cells. However, there was no statistical difference on day 7 measurement of metabolic proficiency (**Figure 7**). This is especially significant as the total protein assay showed a significant difference in the level of protein on day 7 in TCP compared to OPC. This suggests that there may be fewer cells on OPC, but they are more metabolically, active especially in production of ATP (**Figure 7**).

Function: Transferrin & CYP activity

Transferrin synthesised in the liver is important in maintenance of iron homeostasis. Therefore, a functional hepatocyte should show presence of transferrin.

Immunocytostaining showed diffuse staining in isolated cells cultured on TCP, whereas clear, localised, transferrin staining was seen within clusters of cells on OPC.

Over 50 different isoforms of cytochrome P450 enzymes have been identified in the liver. Of these, CYP3A4 is responsible for the metabolism of most xenobiotics. To produce a high level of CYP3A activity in HepaRG™ cultures usually requires induction with DMSO.²⁷ As such, HepaRG™-P cells staining positive for CYP3A4 within a system where DMSO is not used, would be indicative of a functional cell, capable of metabolic enzymatic activity, not usually seen in non-induced cultures.

Immunocytostaining and qRT-PCR for CYP3A4 on day 7 showed high expression and activity in OPC compared to TCP (**Figure 9**). Little to no staining was seen on TCP at day 7, while highly localized staining was seen on OPC at the same time point. qRT-PCR data also showed an almost 80-fold increase of CYP3A4 activity in OPC at day 7 relative to untreated control.

The hypothesis that there would be no difference between cells cultured on OPC and TCP, was disproven. Cells cultured on OPC showed earlier proliferation, differentiation and function as compared to culture on TCP. OPC could therefore not be used to control for the effect of surface treatment for investigation of NPS versus TCP, since NPS were also OPC-treated. We therefore directly compared culture of HepaRG-P in the absence of DMSO on OPC and NPS.

Nanopatterned substrates

The roughness of surfaces has been shown to have varying effects on cell culture enhancing cell cultures under certain conditions while inhibiting adhesion in others.^{7,9} Although analysis of phenotype and function showed an unexpected progression of

differentiation and maturation of cells grown on OPC, we continued to test our second hypothesis attempting to find a NPS which would further enhance adhesion, proliferation and possibly accelerate differentiation in the absence of DMSO compared to OPC.

Mesenchymal stem cells grown on nanopatterned topography exhibited expression of bone relevant markers without the use of additional chemicals or nutrients in the cell media.⁹ The conclusion from this study suggested that surface patterning could direct stem/progenitor-like cells into specific lineages without the need of supplements to stimulate differentiation. Schernthaner (2012)²⁸ also showed evidence that the orientation of patterned surfaces resulted in morphological changes and directional cell alignment along wall like structures. In other studies cell migration has been directed by altering the likelihood of cell adhesion by modifying the form of a nanopattern.²⁹

We tested growth and differentiation of HepaRG™-P cells on 21 different nanopatterned topographies to determine if lineage specific commitment could be directed by the pattern alone. Daily microscopy for adherence and morphology showed that by d7 cells grown on DSQ120 in DMSO-free media showed increased confluency and hepatic morphology compared to any other pattern. All surfaces were oxygen plasma treated before nanopatterning. It might therefore have been expected that all patterned surfaces would be at least as good as OPC without patterning. However, interestingly, only DSQ120 appeared to affect differentiation of HepaRG™-Ps while other patterns had a detrimental effect to the cells. It is possible that pattern distribution/topography and cell type are co-dependent in affecting differentiation on surface architecture. For example, differentiation of MSCs in the absence of chemical direction occurred only on DSQ50.

Morphology and polarity

Particular interest was paid to the first week of culture when we had seen mature hepatocytes emerging in DMSO-free media on OPC. Using NPS we saw increased confluency and cuboidal hepatocyte-like cells on one particular pattern, DSQ120 compared to other patterns and to TCP (**Figure 3**). Cells cultured on DSQ120 showed localised membrane staining for ZO-1 as was seen using OPC, rather than diffuse staining seen on TCP. Suggesting DSQ120 induced early polarisation of membranes comparable to that seen on OPC.

SOX9/HNF4 α reciprocal expression

Immunostaining showed HepaRG™-Ps cultured on OPC and TCP showed reciprocal expression of SOX9 and HNF4 α whereby SOX9 appeared up to day 6 and HNF4 α emerged around day 14. When cultured on DSQ120 showed clear but diffuse expression of HNF4 α at the earlier time of day 6 compared to day 14 when cultured using OPC or TCP (**Figure 5**). This suggests that cells cultured on DSQ120 mature faster than those grown on other substrates. However, the fold change in expression of from qRTPCR data was significantly higher for cells cultured on OPC than either DSQ120 when compared to TCP control (**Figure 6**). The apparent difference seen between staining and qRTPCR data may be due to the difference in gene expression vs the emergence of the functional protein.

Function: Transferrin and CYP3A4 activity

Staining for transferrin and CYP3A4 on DSQ120 showed no difference to OPC, but still out-performed TCP. Similarly, qRTPCR showed no difference between OPC and NPS, though both out-performed TCP. Again, pattern does not seem to play a role in function when compared to oxygen plasma alone, but oxygen plasma significantly outperforms TCP (**Figure 9**).

Viability: Total ATP and metabolic function

Total ATP and PrestoBlue™ assays, of cells cultured on DSQ120, revealed a similar trend to that seen for HepaRG™-P's cultured on OPC. ATP was significantly higher on DSQ120 than TCP, but not different from OPC. PrestoBlue™ data still showed no statistical difference between any condition, but both DSQ120 and OPC showed higher viability than TCP. This suggests that pattern does not play a role in viability, but oxygen plasma significantly increases viability and metabolic competence of cells in culture.

1.1 Conclusion

In this study we have shown that the crucial factor that improved early differentiation and function of the HepaRG™-P cells in the absence of DMSO was oxygen plasma treatment compared to traditional culture methods. DSQ120 nanopatterning of plates promoted differentiation and function comparable to unpatterned oxygen plasma treated plates and was therefore better than TCP. The other nanopatterned substrates studied were inferior in terms of inducing a functional phenotype. It is therefore likely that the beneficial effect seen using the nanopattern substrate was primarily due to oxygen treatment. It is possible that the DSQ120 substrate could

up-regulate specific metabolic enzymes or pathways not investigated in our model compared to OPC and further work could be done to investigate how long cells would remain differentiated in the absence of DMSO and what effect the polymer may have had on the cell culture.

Oxygen plasma treatment of surfaces is relatively inexpensive and could substantially reduce the time and costs of differentiating progenitor cells on traditional culture systems, producing early differentiation and functionality of HepaRG™-P cells and removing the requirement for chemical induction which may have down-stream effects .

References:

1. Lübberstedt et al., 2011. HepaRG human hepatic cell line utility as a surrogate for primary human hepatocytes in drug metabolism assessment in vitro. *Journal of Pharmacological and Toxicological Methods*, 63(1), pp.59–68.
2. Nelson, L., Morgan, K., Treskes, P., Samuel, K., Henderson, C., LeBled, C., Homer, N., Grant, HM., Hayes, PC., Plevris, J., 2017. Human Hepatic HepaRG Cells Maintain an Organotypic Phenotype with High Intrinsic CYP450 Activity/Metabolism and Significantly Outperform Standard HepG2/C3A Cells for Pharmaceutical and Therapeutic Applications. *Basic & Clinical Pharmacology & Toxicology*, 120(1), 30-37.
3. Pal, R., Marmidi, K., Kumar Das, A., Bhonde, R., 2012. Diverse effects of dimethyl sulfoxide (DMSO) on the differentiation potential of human embryonic stem cells, *Archives of Toxicology*, 86 (4) 651-661
4. Czysz, K., Minger, S., and Thomas, N., 2015. DMSO efficiently downregulates pluripotency genes in human embryonic stem cells during definitive endoderm derivation and increases the proficiency of hepatic differentiation. *PLOS one*, 10(2):
5. Park, Y., Smith, R.D., Combs, A.B., Kehrer, J.P., 1988. Prevention of acetaminophen-induced hepatotoxicity by dimethyl sulfoxide, *Toxicology* 14;52(1-2): 165-75
6. Ryan J.A., 2008. Evolution of cell culture surfaces. *BioFiles*3, 21, Sigma-Aldrich/Merck <https://www.sigmaaldrich.com/technical-documents/articles/biofiles/evolution-of-cell.html> (accessed January 2019).
7. Wan, Yuqing et al., 2004. Characterization of surface property of poly(lactide- co-glycolide) after oxygen plasma treatment. *Biomaterials*, 25(19), pp.4777–4783.
8. Lerman, MJ., Lembong, J., Muramoto, S., Gilen, G., and Fisher, JP. 2018 The Evolution of Polystyrene as a Cell Culture Material. *Tissue Engineering Part B: Reviews* Vol. 24, No. 5

9. Dalby, M., Gadegaard, N., Tare, R., Andar, A., Riehle, P H., Wilkinson, C., and Oreffo, R., 2007. The control of human mesenchymal cell differentiation using nanoscale symmetry and disorder. *Nature Materials*, doi:10.1038/nmat2013
10. Curtis, ASG., Gadegaard, N., Dalby, MJ., Riehle, MO., Wilkinson, CDW., Aitchison, G., 2004., Cells react to nanoscale order and symmetry in their surroundings. *NanoBioscience, IEEE Transactions on*, 3(1), pp.61-65
11. Huethorst, E. Cutiongco, Marie F A , Campbell, Fraser A , Saeed, Anwer , Love, Rachel , Reynolds, Paul M , Dalby, Matthew J , Gadegaard, Nikolaj. 2019. Customizable, engineered substrates for rapid screening of cellular cues. *Biofabrication*, pp.Biofabrication, 29 November 2019.
12. Celeen, L., De Spiegelaere, W., David M., De Craene, J., Vinken, M., Vanhaecke, T., Rogiers, V., 2011. Critical selection of reliable reference genes for gene expression study in the HepaRG cell line, *Biochemical Pharmacology*, Vol 81(10), pp.1255-1261
13. Hart, S., Li, Y., Nakamoto, K., Subileau, E., Steen, D., & Zhong, X., 2010. A comparison of whole genome gene expression profiles of HepaRG cells and HepG2 cells to primary human hepatocytes and human liver tissues. *Drug Metabolism and Disposition: The Biological Fate of Chemicals*, 38(6), 988-94.
14. Kawaguchi, Y., 2013. Sox9 and programming of liver and pancreatic progenitors. *Journal Of Clinical Investigation*, 123(5), pp.1881–1886.
15. Hine, R., & Martin, E., (Eds.), 2016. *A Dictionary of Biology: Transferrin*. Oxford University Press. Retrieved 12 Apr. 2018, from <http://www.oxfordreference.com.ezproxy.is.ed.ac.uk/view/10.1093/acref/9780198714378.001.0001/acref-9780198714378-e-4498>.
16. Vandesompele, J., De Preter, K., Pattyn F., Poppe, B., Van Roy, N., De Paepe, A., and Speleman, F. 2002. Accurate normalization of realtime quantitative RT-PCR data by geometric averaging of multiple internal control genes. *Genome Biology* 3(7) Research 0034.1-0034.11
17. Bustin, SA., Benes, V., Garson, JA., Hellemans, J., Huggett, J., Kubista, M.,

- Mueller, R., Nolan, T., Pfaffl, MW., Shipley, GL., Vandesompele, J., Wittwer, Carl T., 2009. The MIQE guidelines: minimum information for publication of quantitative real-time PCR experiments. *Clinical chemistry*, Vol.55(4), pp.611-22
18. Tsai & Lin, 2009. Modulation of morphology and functions of human hepatoblastoma cells by nano-grooved substrata. *Acta Biomaterialia*, 5(5), pp.1442–1454.
19. National Center for Biotechnology Information, SOX9, U.S. National Library of Medicine 8600 Rockville Pike, Bethesda MD, 20894 USA, Accessed March 18, 2018 at <https://www.ncbi.nlm.nih.gov/gene?Db=gene&Cmd=ShowDetailView&TermToSearch=6662>
20. Poncy, A., Antoniou, A., Cordi, S., Pierreux, C.E., Jacquemin, P., Lemaigre, F.P. 2015. Transcription factors SOX4 and SOX9 cooperatively control development of bile ducts, *Developmental Biology*, Vol 4 (2) 136-148
21. Antoniou, A., Raynaud, P., Cordi, S., Zong, Y., Tronche, F., Stanger, B.Z., Jacquemin, P., Pierreux, C.E., Clotman, F., Lemaigre, FP., 2009. Intrahepatic bile ducts develop according to a new mode of tubulogenesis regulated by the transcription factor SOX9, *Gastroenterology* 136 (7) 2325-2333
22. Ahn, M., Shah, YM., Inoue, J., Morimura, K., Kim, I., Yim, S., Lambert, G., Kurotani, R., Nagashima, K., Gonzalez, FJ., Inoue, Y., 2008. Hepatocyte nuclear factor 4 α in the intestinal epithelial cells protects against inflammatory bowel disease. *Inflammatory Bowel Diseases*, 14(7), 908-920.
23. Babeu, JP. and Boudreau, F., 2014. Hepatocyte nuclear factor 4-alpha involvement in liver and intestinal inflammatory networks, *World Journal of Gastroenterology* Vol 20(1), p22-30
24. Bonzo, J.A., Ferry, C.H., Matsubara, T., Kim, JH. and Gonzalez, FJ., 2012. Suppression of Hepatocyte Proliferation by Hepatocyte Nuclear Factor 4 α in Adult Mice, *Journal of Biological Chemistry* Vol. 287 (10) pp 7345-56
25. Guillaume F. and Otto SP., 2012. Gene Functional Trade-Offs and the Evolution of Pleiotropy. *Genetics*. 192(4):1389-1409.
doi:10.1534/genetics.112.143214

26. Matsuo, S., Ogawa, M., Muckenthaler, M.U., Mizui, Y., Sasaki, S., Fujimura, T., Takizawa, M., Ariga, N., Oaki, H., Sakaguchi, M., Gonzalez, F.J., and Inoue, Y., 2015. Hepatocyte Nuclear Factor 4 α Controls Iron Metabolism and Regulates Transferrin Receptor 2 in Mouse Liver. *J Biol Chem.* 290(52): 30855-30865
27. Guguen-Gouillozo, C., Corlu, A., and Gouillozo, A., 2010. Stem cell derived hepatocytes and their use in toxicology, *Toxicology* 270(1) 3-9
28. Schernthaner, M., Reisinger, B., Wolinski, H., Kohlwein, S., Trantina-Yates, A., Fahrner, M., Romanin, C., Itani, H., Stifter, D., Leitinger, G., Groschner, K., and Heitz, J., 2012. Nanopatterned polymer substrates promote endothelial proliferation by initiation of B-catenin transcriptional signalling. *Acta Biomaterialia* 8 : 2953-2962
29. Qian, T. and Wang, Y., 2010. Micro/nano-fabrication technologies for cell biology, *Med Bio Eng Comput* 48:1023-1032

Acknowledgements:

Author Disclosure Statement:

All authors declare no conflict of interest.

Corresponding Author:

Katie Morgan

Hepatology Laboratory

University of Edinburgh

Royal Infirmary of Edinburgh,

Chancellor's Building

49 Little France Crescent

Edinburgh EH16 4SB (UK)

07725216902

Degree: PhD

Figures & Tables:

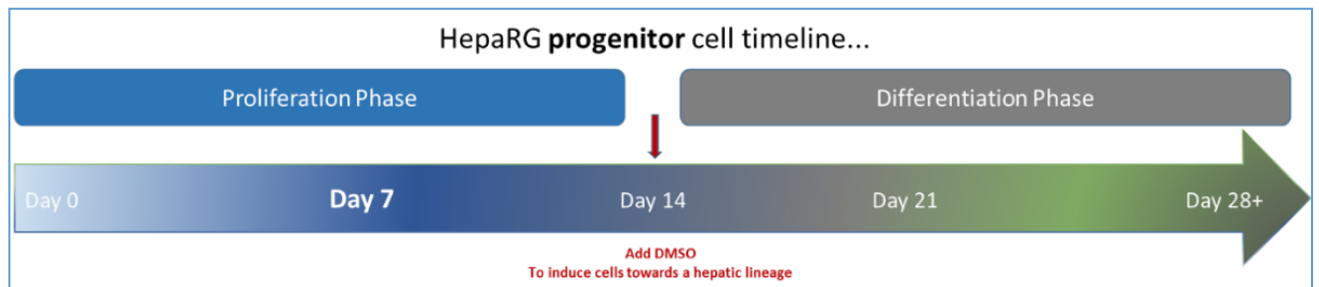


Figure 1: Timeline for proliferation and differentiation of HepaRG-P™ on TCP. Showing distinct phases defined by day 14 change to medium supplemented with DMSO for induction and sustained commitment of hepatocytes .

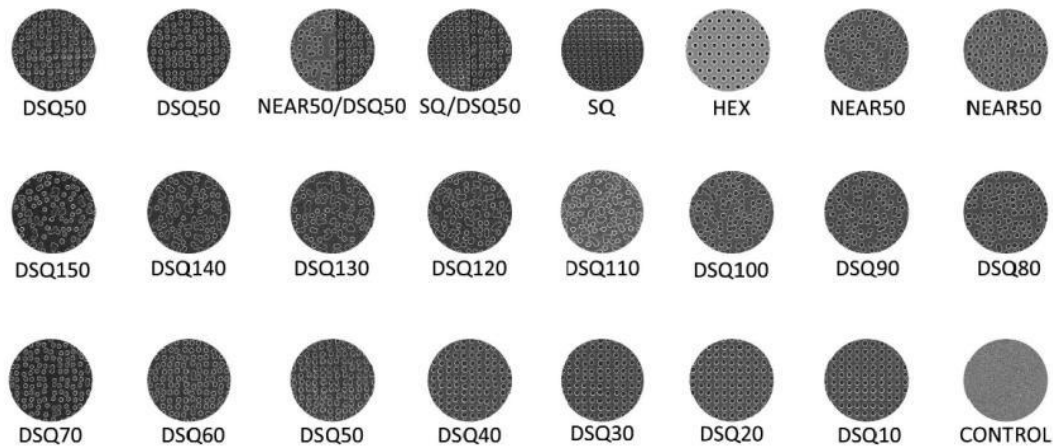


Figure 2: Illustration of nanopatterned slide

Slides were oxygen plasma coated before application of nanopatterns. Wells were based on a standard 96 well plate format and included an unpatterned control well, 21 different nanopatterns and duplicates of DSQ50 and Near50. The gradient from DSQ10 to DSQ150 allowed for assessment of nanotopographical sensitivity of the cells.

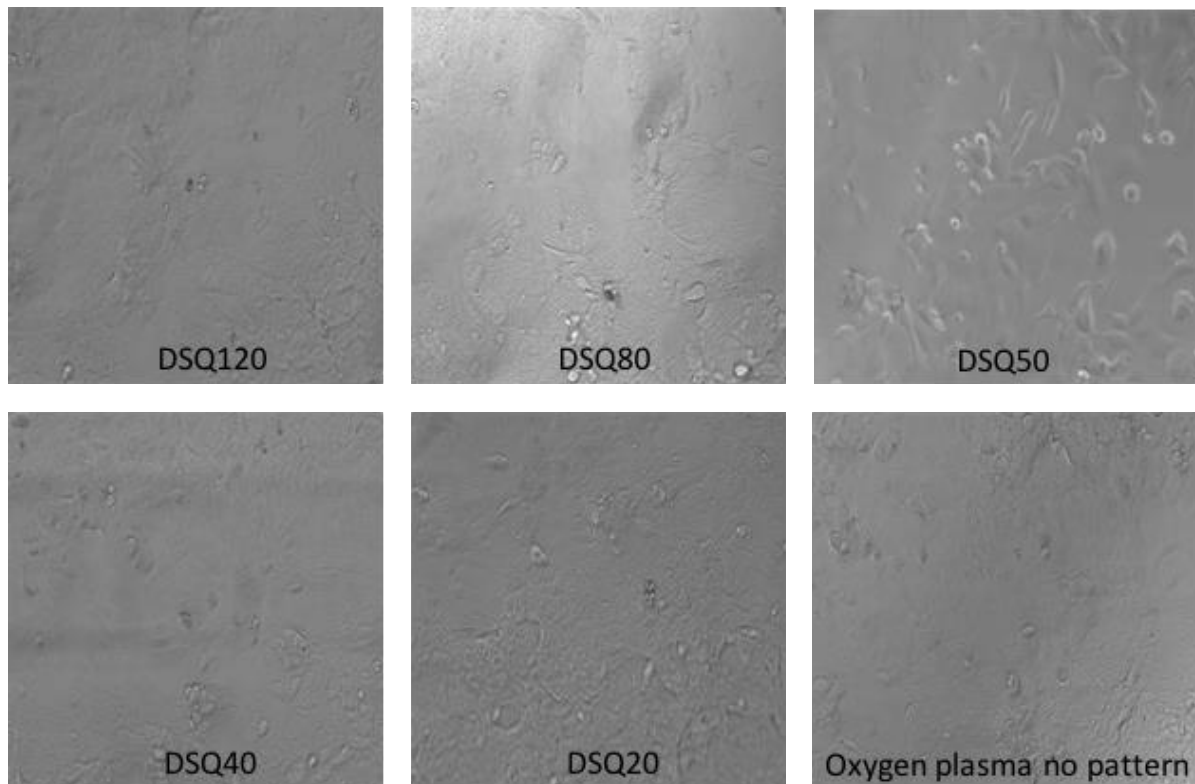


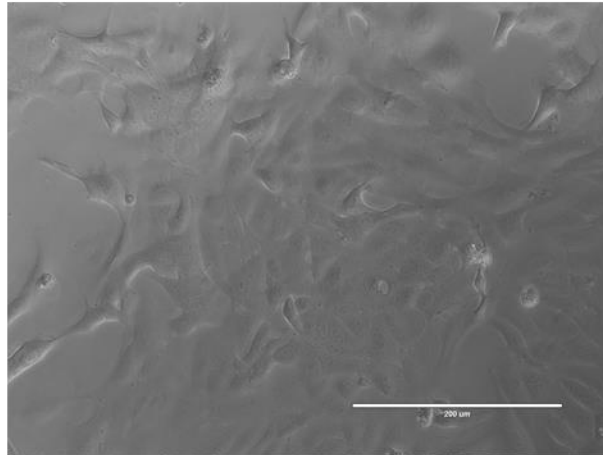
Figure 3: Morphology of HepaRG-P cells seeded on nanopatterned and oxygen plasma treated surfaces:

Growth of HepaRG-P grown on selected nanopatterns in DMSO free medium showing differences in confluency and maturity of culture. Oxygen plasma treated surface with no pattern shows confluency and some cuboidal cells. On DSQ50 and 40 cultures were non-confluent progenitors with no cuboidal cells. Cultures on DSQ20 and 80 had a ragged appearance and were not confluent. Though DSQ20 seemed to have some cuboidal cells, it did not meet all criteria for inclusion in this study. HepaRG-P cells cultured on DSQ120 were confluent with some cuboidal cells, indicative of hepatocyte lineage, and their morphology was the only pattern comparable to that on the unpatterned oxygen plasma treated surface.

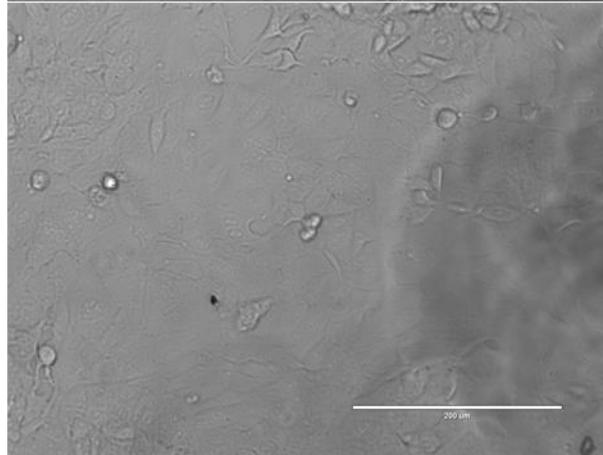
Images acquired using an EVOS Auto FI (x20, line measures 200 μ m)

Day 6

TCP



OPC



DSQ120

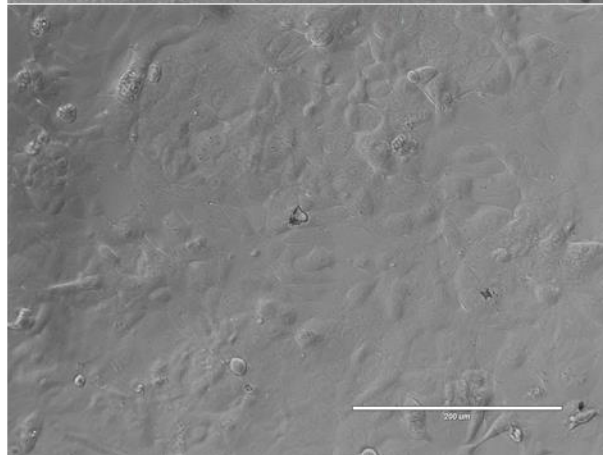
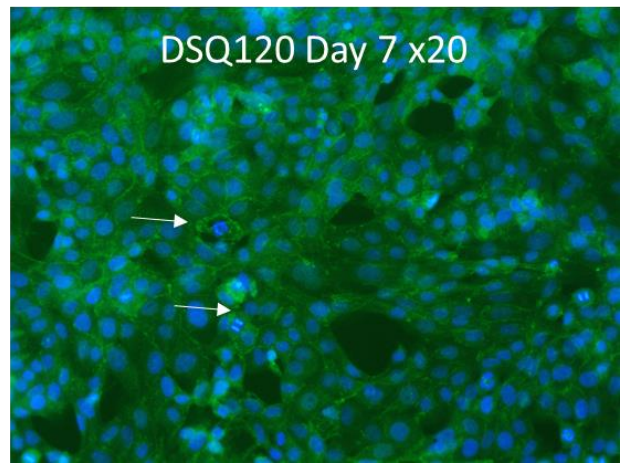
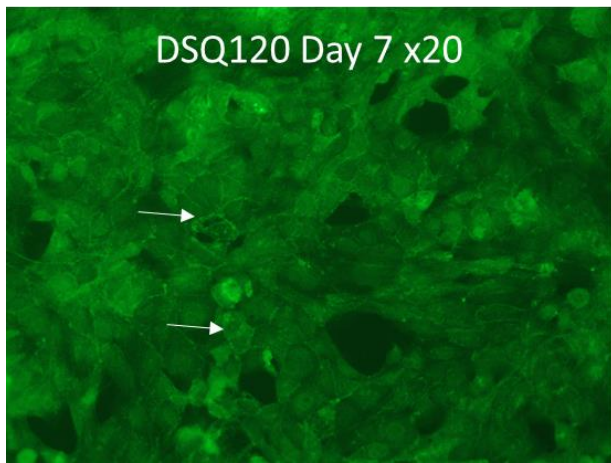
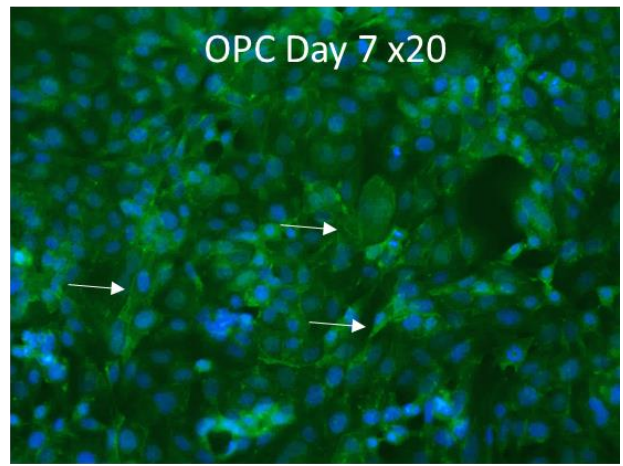
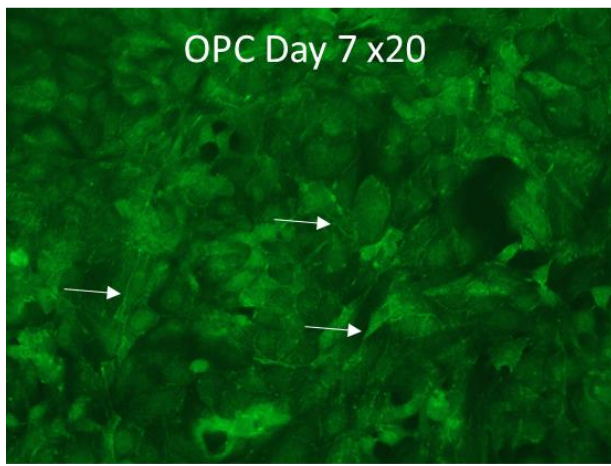
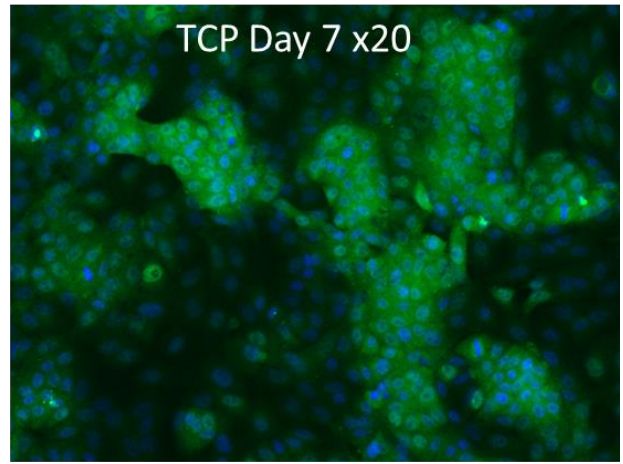
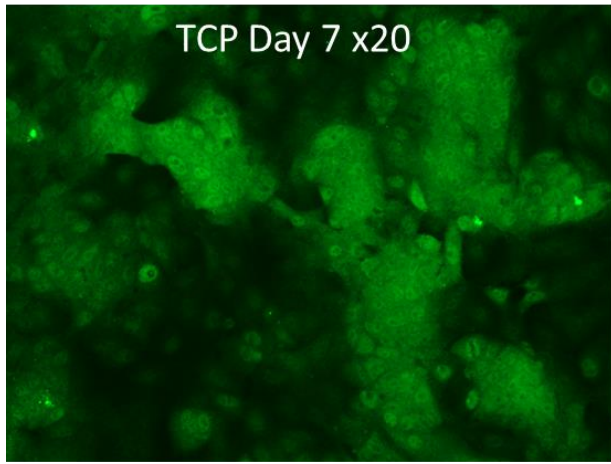


Figure 4: Morphological assessment of HepaRG™-P cells cultured on TCP, OPC and DSQ120 at day 6.

Phase contrast microscopy showing HepaRG™-P cells at day 6 of culture. Confluency was lower on TCP (96w Corning) than OPC (Oxygen plasma coated control) and DSQ120 (nanopatterned substrate). On OPC cells were smaller compared with those on TCP and on NSP cells with cuboidal morphology indicative

of hepatocytes can be seen. Images acquired using an EVOS Auto FI (x20, scale bar measures 200 μ m)

A)



B)

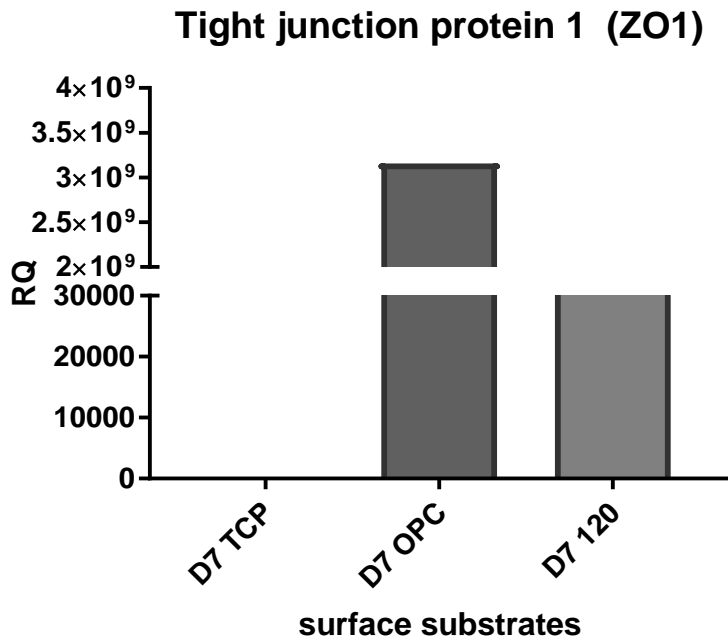


Figure 5: Staining and qRT-PCR for Zonular Occludens 1 a marker of cellular polarity:

A) Zonular Occludens 1 staining: HepaRG™-P cells were grown for 7 days on OPC, DSQ120 and TCP. Cells were fixed and stained on day 7 for Hepatic polarity marker Zonular Occludens 1 (ZO-1, green) and nuclei were stained with Hoescht (blue). Cells cultured on TCP showed dispersed cytoplasmic expression, while those on OPC and DSQ120 showed localized membrane bound ZO-1 ('chicken wire' appearance) and formation of bile canaliculi typically seen in a mature HepaRG™. Images acquired using an EVOS Auto FI (x20, scale bar measures 200µm)

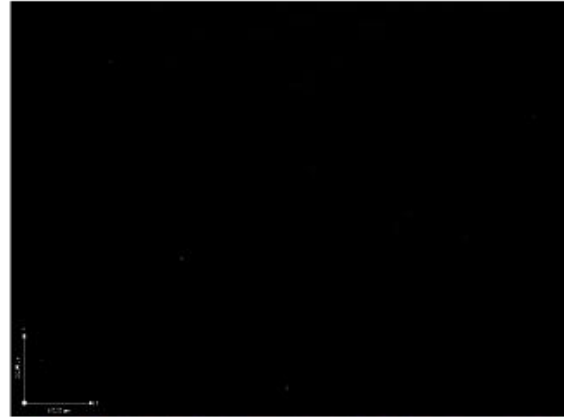
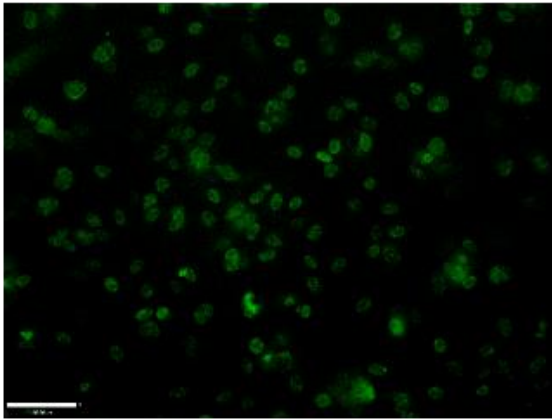
B) qRT-PCR of Tight Junction Protein 1 (TJP1) the gene encoding for ZO-1 protein: Expression of TJP1 correlated with ZO-1. Very low to none for cells cultured on TCP, and significant increases of xxxfold and xxxfold on OPC and NCP respectively. Fold-changes were calculated relative to untreated control by the $\Delta\Delta Cq$ method. (n=3, representing 3 independent experiments with 3 technical replicates each experiment).

A DSQ120

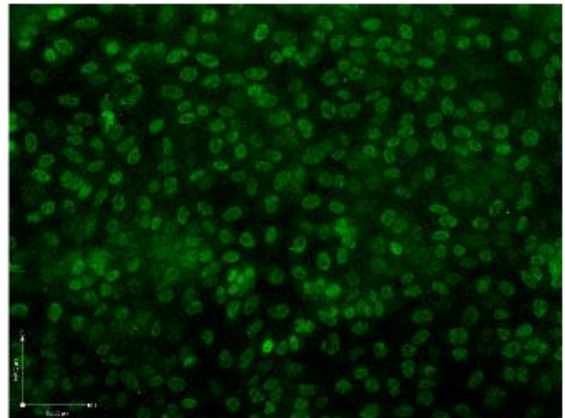
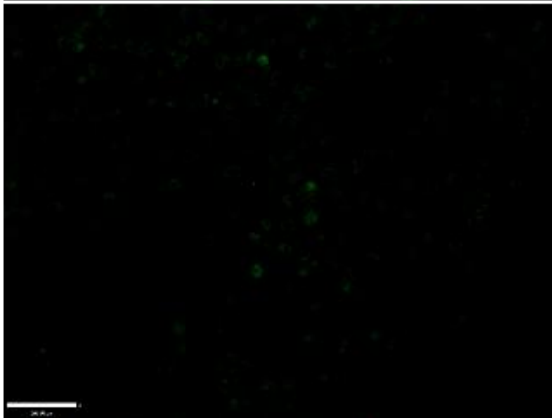
Sox 9

HNF4 α

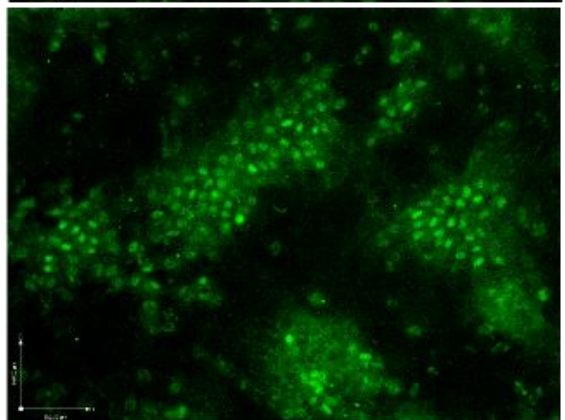
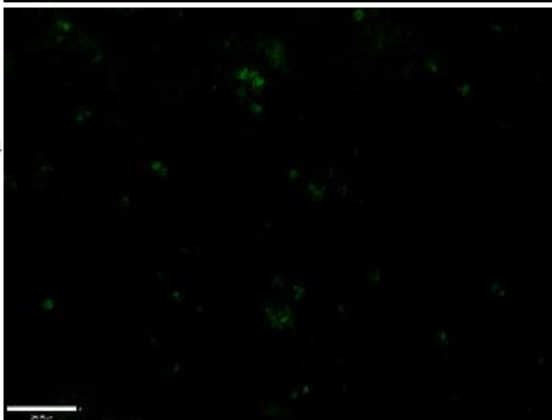
Day 2



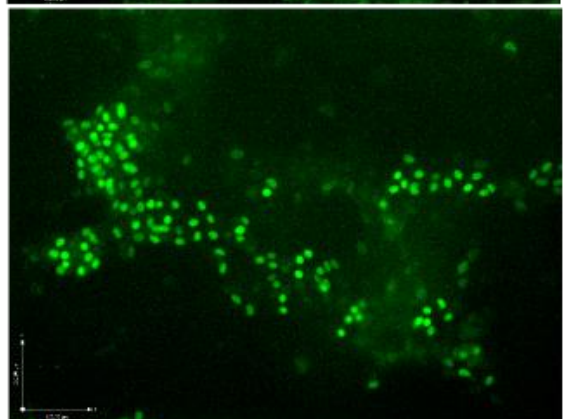
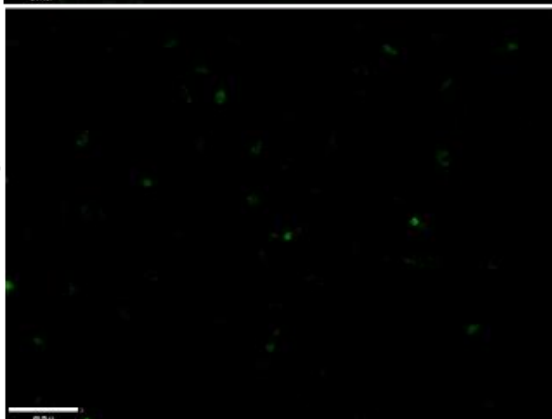
Day 6



Day 14



Day 28

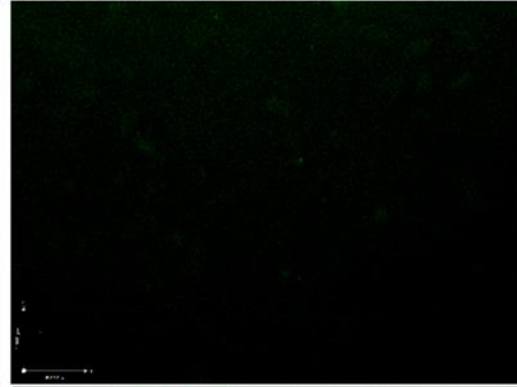
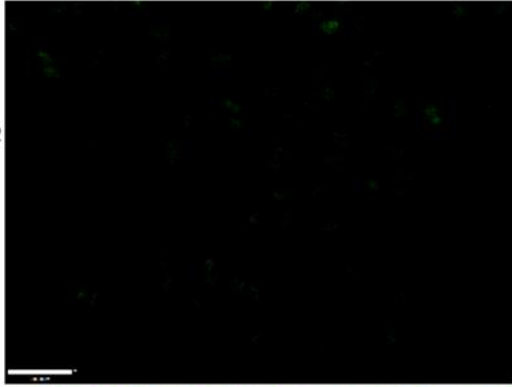


B UP

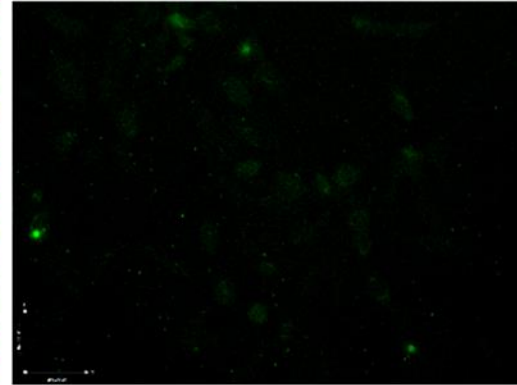
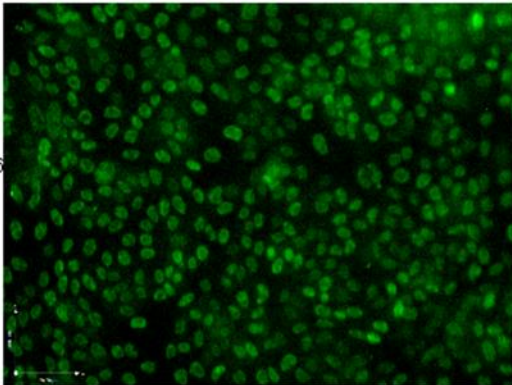
Sox 9

HNF4 α

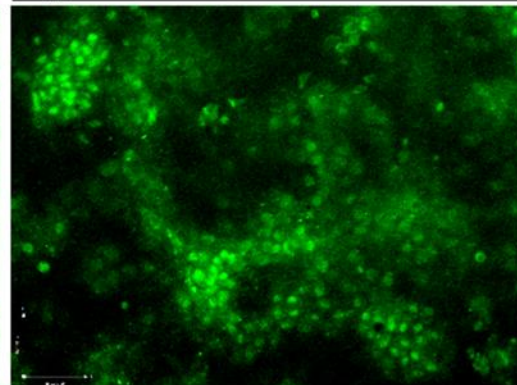
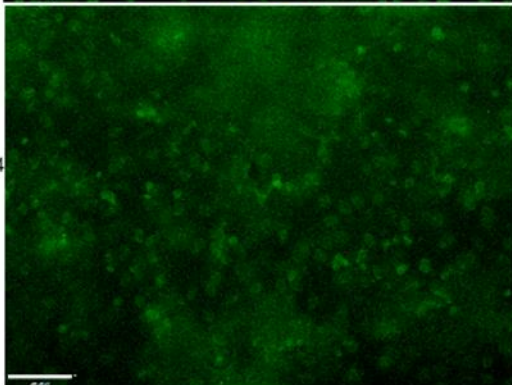
Day 2



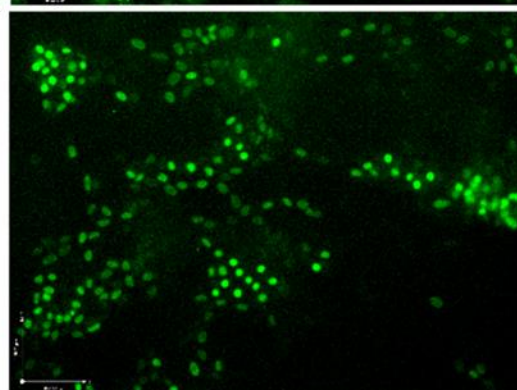
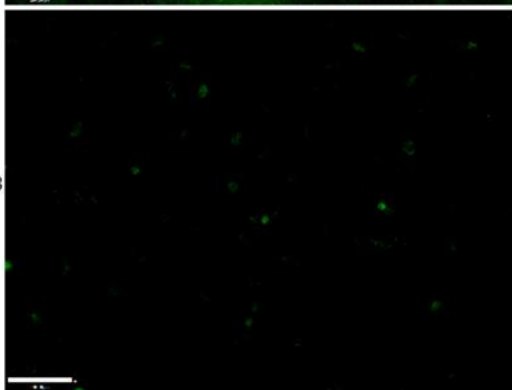
Day 6



Day 14



Day 28



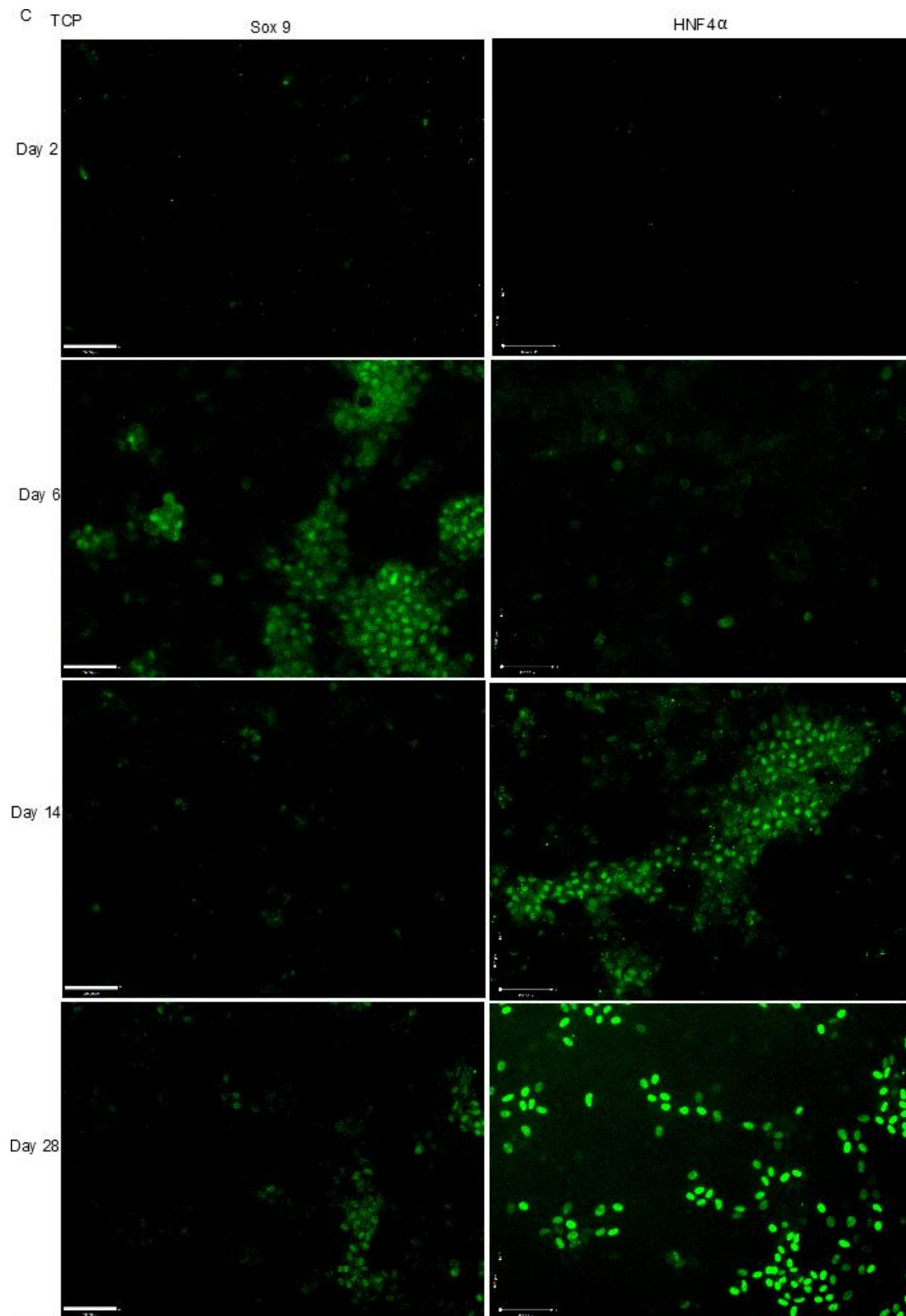


Figure 6: Phenotypic staining for progenitor protein SOX9 and mature hepatocyte marker HNF4 α : All surfaces showed reciprocal staining of SOX9 and HNF4 α throughout a 28 day culture period.

Sox9: Cytoplasmic Sox9 staining (green) was only seen at day 2 on DSQ 120 (A) and was lost by d6. For TCP (C) and OCP (B) localised and brighter sox9 expression was detected at d6. By d14 staining was diffuse on OCP and lost from TCP. by d28 it was no longer detectable on OCP and had reappeared on some cells on TCP.

HNF4 α : early diffuse expression was seen by d6 only on DSQ120 This became more localised by d14 when it was comparable to TCP and OCP. Expression persisted at d28. Images acquired using an EVOS Auto FI (x20, line measures 160 μ m). Background fluorescence was subtracted across all images equally using Volocity image analysis software (Perkin Elmer).

A No expression of Sox 9

B

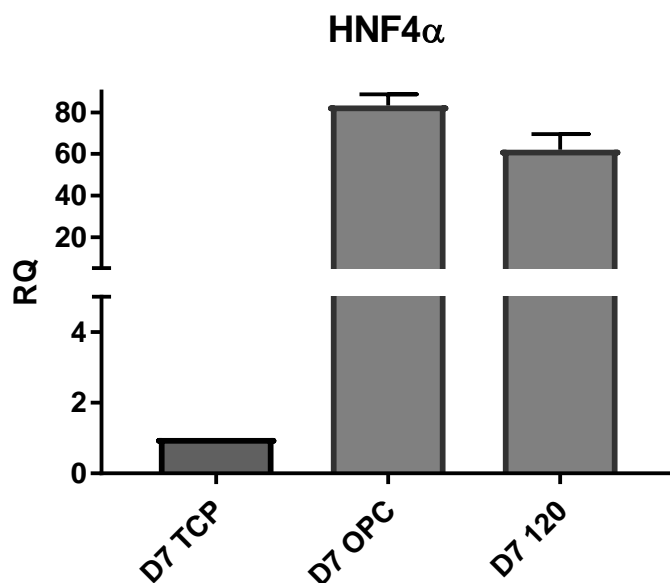


Figure 7: qRTPCR data for Sox9 and HNF4 α day 7:

A) No expression of SOX9 was detected on any substrate (n=6).

B). Both OPC and DSQ120 showed higher levels of mRNA expression on day 7 than TCP.

Fold-changes were calculated relative to untreated control by the $\Delta\Delta$ Cq method. (n=3, representing 3 independent experiments with 3 technical replicates each experiment).

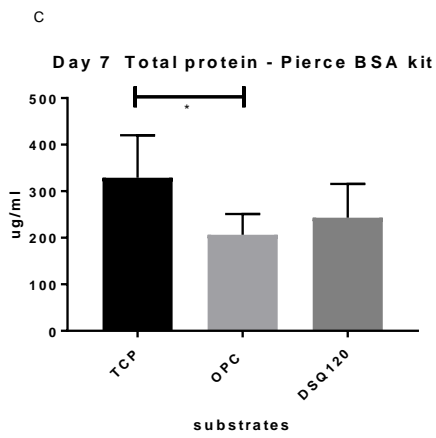
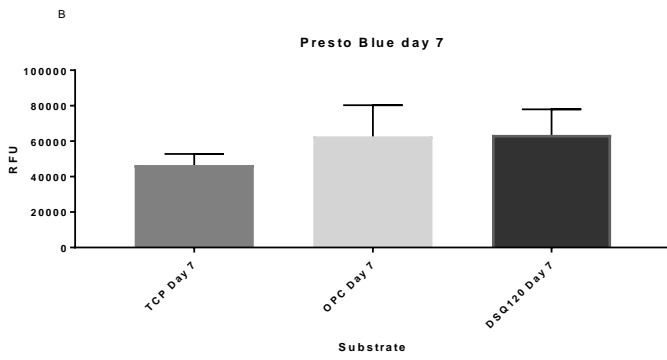
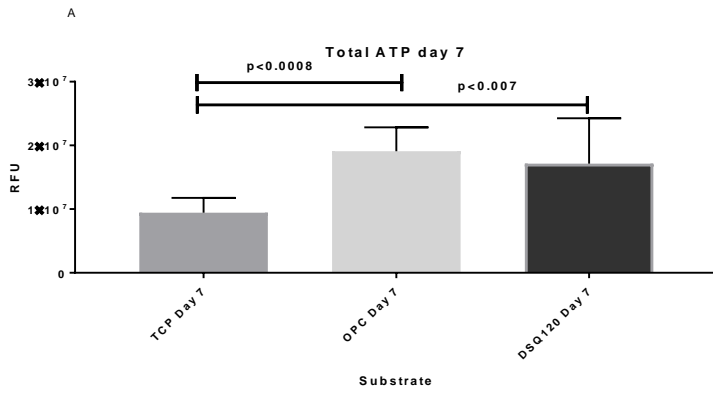


Figure 8: Measuring total ATP in HepaRG™-P cells at day 7 across cell culture substrates:

A) statistically significant differences in ATP were seen between HepaRG™-P cells grown on TCP and both OCP ($p < 0.0008$) and NPS ($p < 0.007$) substrates. There was no significant difference in total ATP comparing cells grown on OPC and DSQ120 patterned surfaces ($n=3$, representing 3 independent experiments with 3 technical replicates each experiment). Data expressed as relative fluorescent units

B) Measuring viability in HepaRG™-P cells at day 7 across cell culture substrates: The PrestoBlue™ resazurin based assay, showed no significant difference between TCP, OPC or NPS DSQ120. ($n=3$, representing 3 independent experiments with 3 technical replicates each experiment). Data expressed as relative fluorescent units

C) Pierce BCA total protein analysis of HepaRG™-P cells at day 7 across all cell culture substrates: At d7 total protein recovered from TCP was significantly higher compared to OPC ($p=0.25$). There was no significant difference between NPS and TCP or NPS. Data comprises 3 experiments with 2 technical replicates each experiment. Technical replicates were pooled from 5 wells for each condition.

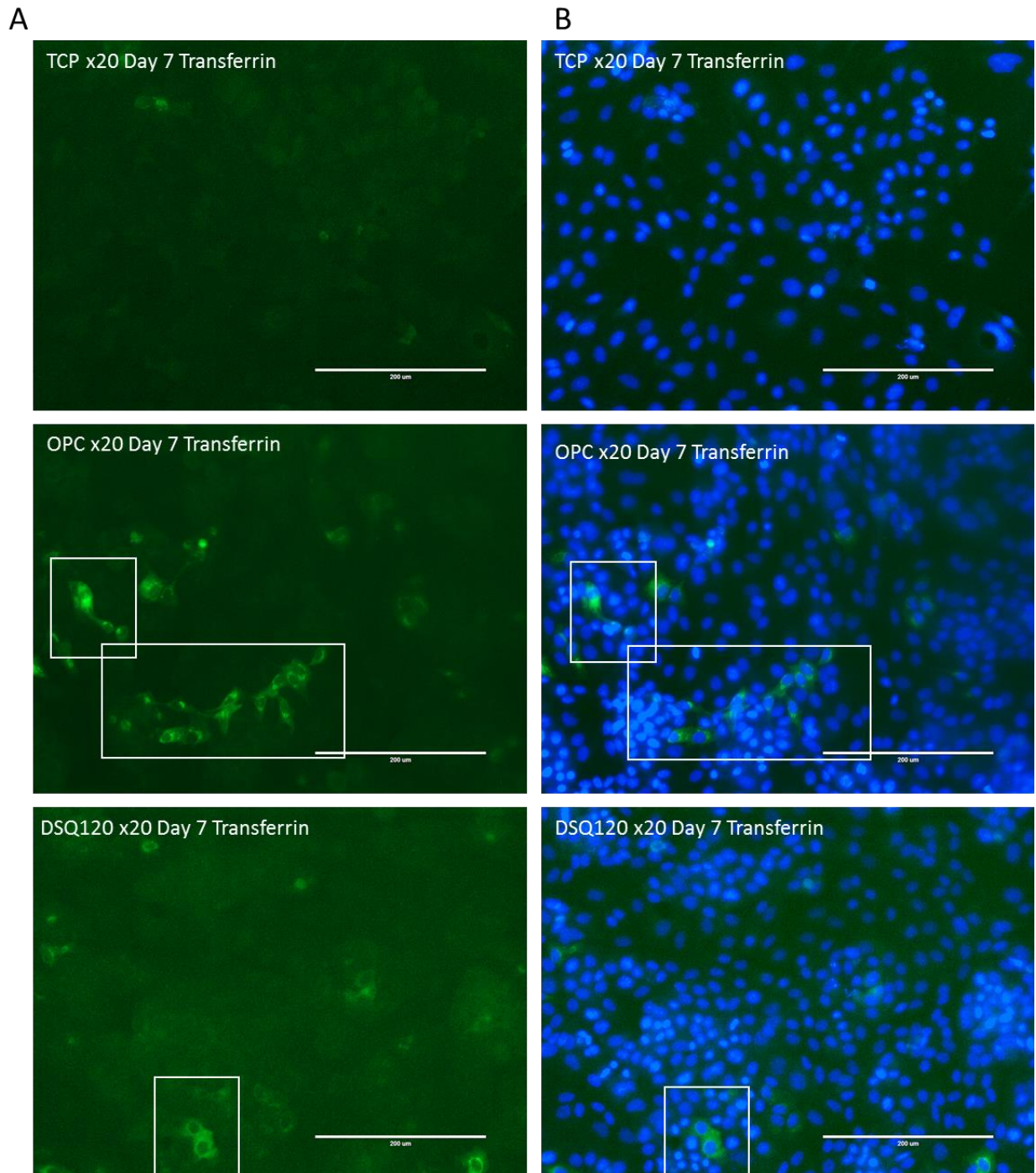
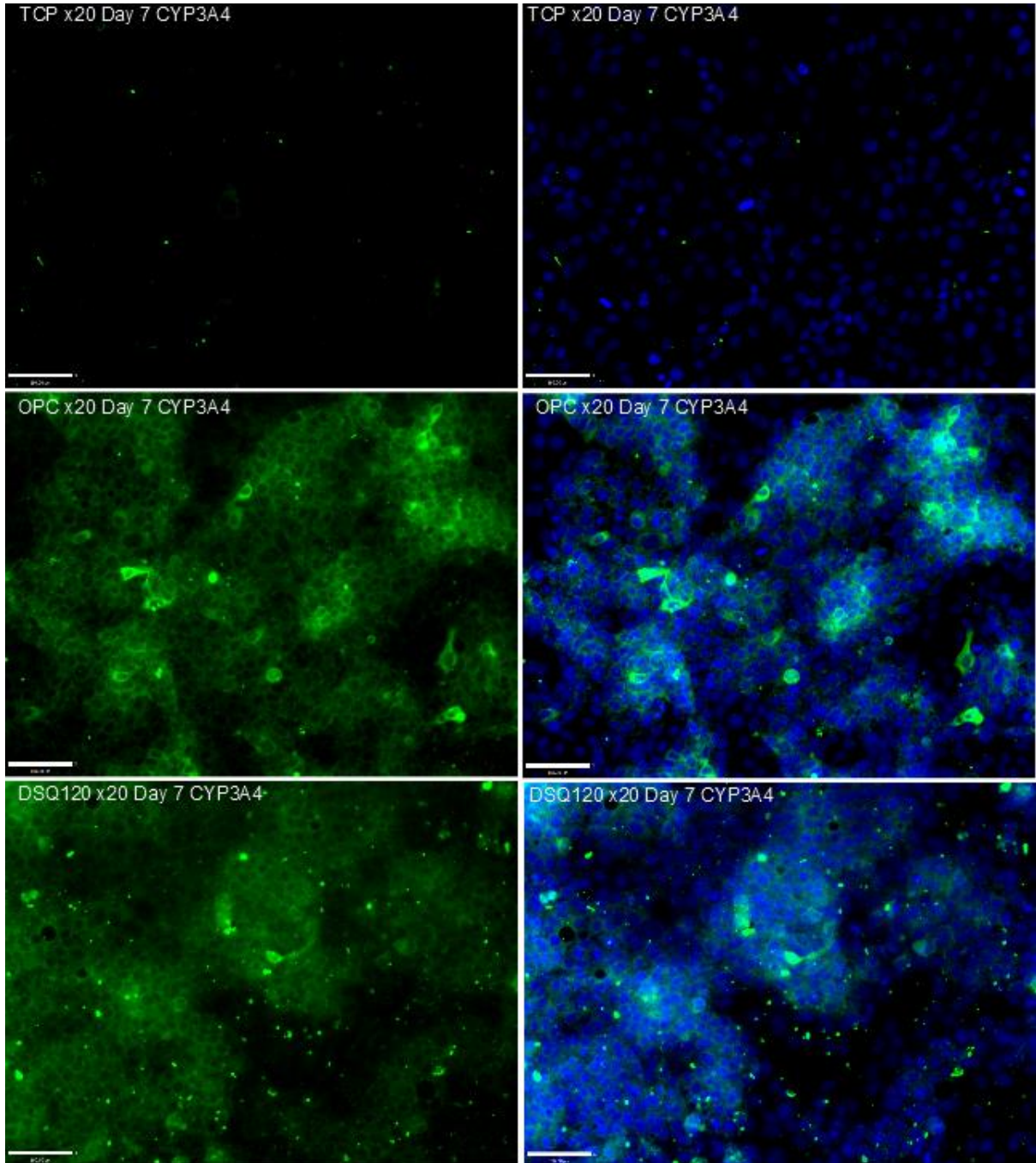


Figure 9: Transferrin antibody staining: A) staining of HepaRG-P™ cells for transferrin (green) showed localized staining on OPC at day 7. There was no to little staining in TCP and DSQ120 respectively and that for DSQ120 was diffuse.

B) Images from panel A overlaid with Hoescht nuclear staining. Representative of n=2 biological with 3 technical replicates. Images acquired using an EVOS Flo Auto (x20, scale bar measures 200 μm). Background fluorescence subtracted across all images equally using Volocity image analysis software (Perkin Elmer).

A)



B)

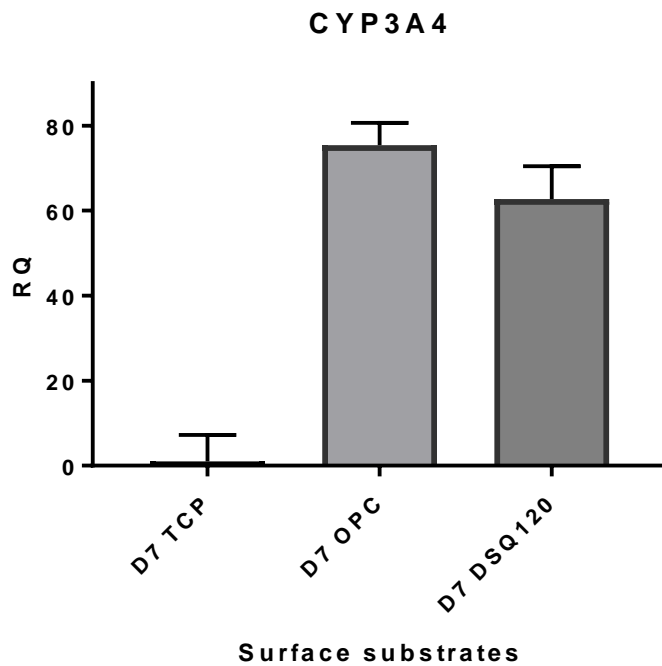


Figure 10: Expression of CYP3A4 using immunocytostaining and qRTPCR to assess function of cultured HepaRG™-P

A HepaRG™-P cells cultured on TCP show little to no **CYP3A4** staining. Clear and abundant localised cytoplasmic staining was seen in OPC and DSQ120.

B) Images from panel A overlaid with Hoescht nuclear staining. (X20 magnification on EVOS Auto-fl microscope) (scale 160µm). Data representative of n=2 biological and 2 technical replicates. Images acquired using an EVOS Flo Auto (x20, scale bar measures 200µm) Background fluorescence subtracted across all images equally using Volocity image analysis software (Perkin Elmer).

B At d7 significant upregulation of CYP3A4 was seen on OPC and DSQ120 compared to TCP. Results are presented as fold-changes in gene expression relative to untreated control calculated with the $\Delta\Delta C_q$ method. (n=3, representing 3 independent experiments with 3 technical replicates each experiment).

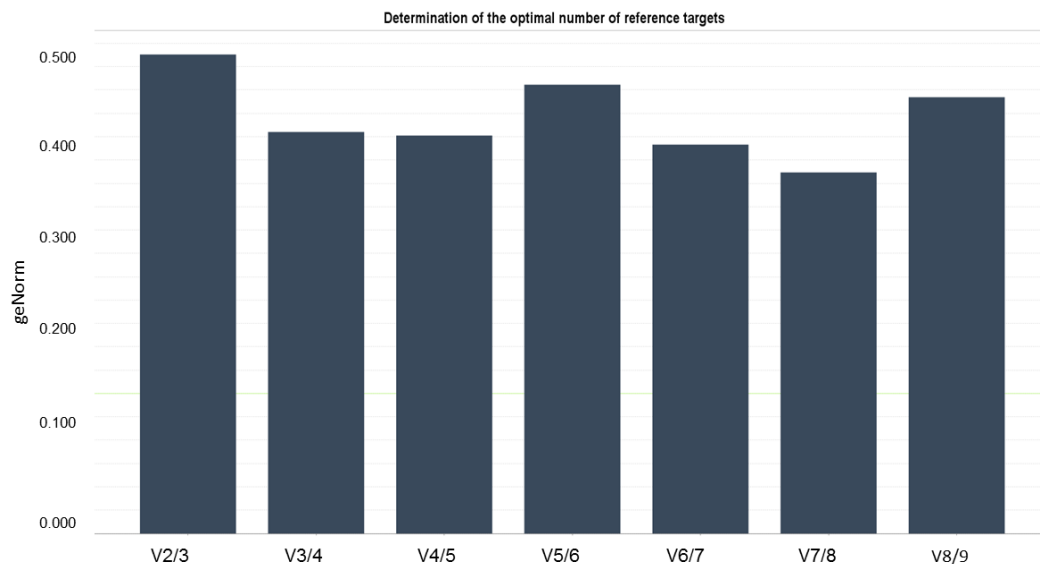
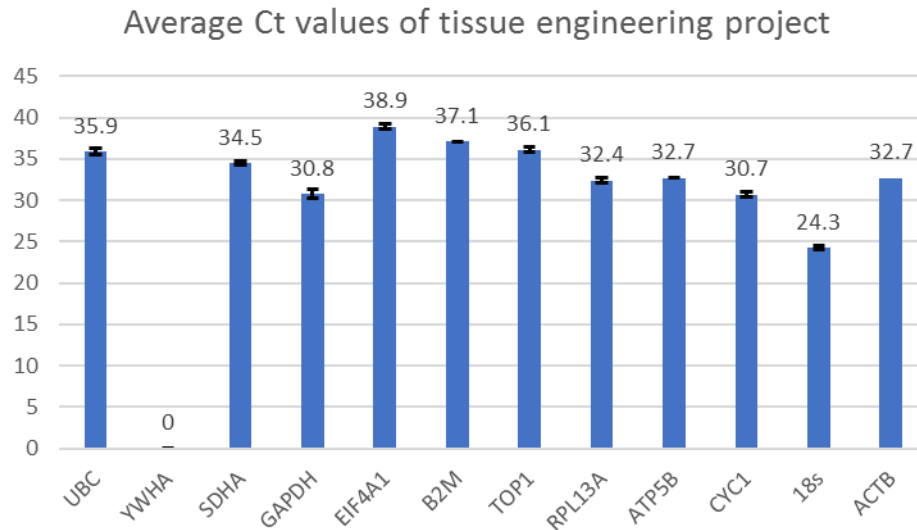


Figure 11: Reference gene analysis: A) Average Ct values for Nanopattern substrate reference gene selection: Average Ct values are shown for all 12 genes used in validating optimal reference genes. SD shown in error bars of SEM.

B) V values generated by geNorm software for Nanopattern project: The optimal number of reference genes is determined by V value from analysis of pairwise variation between all samples. The lower the V value the more optimal the number of reference genes for use in normalisation. In this study a combination of 7/8 reference genes is suggested for use in normalising genes of interest

Table 1

Primary Antibody	Catalogue Number	Dilution
Z01 Santa Cruz Rabbit polyclonal primary antibody	SC 10804	1:50
HNF4a, monoclonal mouse, Abcam Cambridge, UK	Ab41898	1:1000
SOX9 Santa Cruz Rabbit polyclonal antibody	SC20093	1:500
Rabbit-anti-Transferrin FITC –primary antibody, abcam, Cambridge, UK	Ab34670	1:200
CYP3A4 primary antibody, Merck, Millipore Darmstadt, Germany	Ab1254	1:500

Table 1: Dilutions of primary antibodies – Name, product number and manufacturer of primary antibodies used throughout, alongside optimal dilutions.

Table 2: Tested reference genes with names and functions

Abbreviation	Name	Function
18S	18S ribosomal RNA subunit	Component of eukaryotic ribosomal subunit 40S

ATP5b	ATP synthase subunit 5b	Encodes a subunit of mitochondrial ATP synthase
β -Actin	Beta-actin	Isoform of actin proteins – part of cytoskeleton
B2M	Beta-2microglobulin	Encodes a protein found in major histocompatibility protein (MHC) 1
CYC1	Cyclin D1	Encodes a subunit of the mitochondrial transport chain
EIFa2	Eukaryotic initiation factor 4a2	A component of a complex which facilitates recruitment of mRNA to ribosome
GAPDH	Glyceraldehyde-3-phosphate dehydrogenase	Important enzyme for ATP production
RPL13a	Ribosomal protein L13a	Ribosomal subunit
SDHA	Succinate dehydrogenase complex, subunit A	Subunit of succinate dehydrogenase that plays a role in energy

		conversion within mitochondria
TOP1	Topoisomerase 1	Encodes an enzyme responsible for the breaking and subsequent joining of DNA during transcription
UBC	Ubiquitin C	Encodes a polyubiquitin precursor which helps regulate and modify various effects within the cell
YHWAZ	Phospholipase A2	Adapter protein which binds other protein complexes in many signalling pathways

Table: 2 The geNorm output ranked the candidate reference gene according to their expression stability (M).


Reference genes for nanopattern project ranked from most to least stable			
Tissue Engineering			
	Ct value	M value	Reference Gene
Most stable  Least stable	30.7	<1.0	CYC1
	34.5	1	SDHA
	24.3	1.2	18s
	32.7	>1.4	ATP5B
	30.8	1.8	GAPDH
	38.9	2.2	EIF4A1
	35.9	2.5	UBC

Table 3: Reference gene ranking for nanopattern project Ct and M Values generated using geNorm software to identify Reference genes for tissue engineering/nanopattern project using HepaRG™-P cells, ranked in order of most to least stable in according to M value